Ab Initio Molecular Dynamics Simulation of the Interaction between Water and Ti in Zeolitic Systems

Ettore Fois,* Aldo Gamba, and Eleonora Spanò

Dipartimento di Scienze Chimiche Fisiche e Matematiche, Universita' dell'Insubria, and INSTM Udr Como, via Lucini 3, I-22100, Como, Italy

Received: July 10, 2003; In Final Form: October 21, 2003

We present the results of ab initio molecular dynamics simulations on titanium offretite. The aim of this work is to investigate at a microscopic level the room temperature behavior of titanium inserted into a fully periodic zeolitic framework in dry and hydrated conditions. Structural analysis indicates that titanium, at low water loading, is tetrahedrally coordinated by framework oxygens only. On the other hand, at higher loading, when water molecules are activated via hydrogen bonding, they interact with the Ti site, leading to an increase of the Ti coordination number up to 5. The insertion of a Ti center causes only moderate and local distortions to the silicate framework. Features due to Ti in the calculated vibrational spectra are in line with IR and Raman experiments.

1. Introduction

Ti-incorporated zeolites are very interesting materials used as oxidizing catalysts under mild conditions.[1−4] Zeolites[5] are open-framework crystalline structures characterized by molecular-sized cages and channels. The building blocks are TO_4 tetrahedra, where T is generally Si and/or Al. Each cation, Si or Al, is surrounded by four oxygens in a tetrahedral arrangement. Each tetrahedron is connected, by sharing corners, with other four to build a framework structure. Cations, different from Si and Al, may be present in tetrahedral sites in the zeolitic framework; however, it is possible to find extraframework cations as well. Alkaline and alkaline-earth ions are found in both natural and synthetic zeolites, and such extraframework cations occupy positions in the cages and are coordinated by framework oxygens and water molecules as well.[5]

Since the first synthesis of a Ti zeolite,[1] several attempts have been made in order to characterize the structure of the titanium center.[4] It is now established that, at low concentration, Ti occupies tetrahedral sites in the zeolite framework;[4,6] namely, that Ti isomorphously replaces silicon. Several X-ray absorption, extended X-ray absorption fine structure (EXAFS), infrared, Raman, and UV−vis spectroscopic studies[7−17] have shown that tetravalent titanium in microporous silicates may increase reversibly its coordination number from 4 to 5 or even 6 upon exposure to adsorbates. Upon addition of H_2O the 48 000−50 000 cm^{-1} UV−vis band, typical of tetracoordinated Ti, shifts progressively to 42 000 cm^{-1}, and this effect is reversible. Moreover, titanium−adsorbate interactions have been investigated by IR and Raman spectroscopies, where intensity variations and frequency shifts around 960 cm^{-1} (IR and Raman) and 1125 cm^{-1} (Raman) are found.[17]

Water chemisorption at Ti sites can be considered as well: it should involve the breaking of a Ti−O−Si bridge with the formation of silanol or titanol groups. Chemisorption, however, seems to be in contrast with the reversibility found in many experiments.

In typical olefin epoxidation, H_2O_2 is present as an oxygen source and therefore hydrogen peroxide interaction with Ti may be relevant as well. Also, the presence of a potential ligand like OH^- seems to increase reaction rates.[2,18−21]

Beyond experimental investigations, a number of computational studies have been performed.[7,17,22−29] Most of the calculations were performed at 0 K, searching energy minima in cluster configurations. Such investigations converged to a Ti−O distance of about 1.8 Å. Moreover, small energy differences among different geometries, representative of various sites in zeolitic frameworks, have been reported. Comprehensive reviews of such cluster modeling can be found in refs 12 and 24. Also, a series of ab initio studies where the periodic zeolitic framework was taken into account have appeared.[27,28] In ref 28, beyond an updated review of previous studies, the interaction energies of small molecules (H_2O, NH_3, H_2CO, and CH_3CN) with a Ti center in chabasite (Ti-CHA) have been studied by ab initio energy minimization adopting a localized (Gaussian) basis set. Ti, in the bare zeolite, was found in a slightly distorted tetrahedral geometry, while in the molecule−crystal adduct, Ti was found in a trigonal bipyramid arrangement with the ligand's heavier element coordinated to Ti. The stability (binding energy) of the adducts was found in the order $NH_3 > H_2O > H_2CO \approx CH_3CN$ (the relative order of the two latter ligands' binding energies was found to be dependent on the accuracy of the calculations). In the case of H_2O,[28] a binding energy of 48.6 kJ mol^{-1} (25.1 kJ mol^{-1} when corrected for BSSE) and a Ti−water oxygen distance of 2.38 Å were calculated, while the Ti framework oxygen distances vary from 1.790−1.801 Å in the bare Ti chabasite to 1.802−1.825 Å in the optimized geometry of the Ti−CHA−H_2O system.

Water in Ti silicalite has been studied via mixed QM/MM approaches as well, and binding energies ranging from 0 to 31 kJ mol^{-1} have been reported, the actual value depending on the Ti site.[29]

The catalytically most active Ti zeolite is Ti silicalite, TS-1. Silicalite[30] is a silica-rich zeolite with MFI framework topology and chemical formula per unit cell [$Si_{96}O_{192}$]. However, other silica-rich Ti zeolites have been synthesized. Due to the

* Corresponding author: e-mail fois@fis.unico.it; fax ++ 039 031 326230; phone ++ 039 031 326218.

10.1021/jp030834e CCC: $27.50 © 2004 American Chemical Society
Published on Web 11/25/2003

computational cost of the Car−Parrinello[31] ab initio molecular dynamics technique, our attention has been addressed to offretite,[32] a zeolite whose unit cell is smaller than in silicalite. The offretite framework $[T_{18}O_{36}]$ is characterized by 18 tetrahedral cations T (e.g., Si) in the unit cell, with rectilinear 12-ring channels whose diameter is of comparable, even larger, magnitude with respect to the silicalite channels system.[30] However, titanium offretite has been synthesized and its catalytic activity has been reported as well.[33]

In this work, we present results from finite temperature computer simulations on Ti offretite (Ti-OFF) performed in pre-reactive conditions, namely investigations aimed to study at microscopic level the titanium center and its interaction with water.

Three different systems have been examined: an anhydrous titanium offretite $[TiSi_{17}O_{36}]$ (Ti-SiOFF), with 1/18 Ti/T ratio, and two hydrated Ti-SiOFFs with chemical formula per unit cell $[TiSi_{17}O_{36}](H_2O)_2$ with the same Ti/T ratio. The experimental content of Ti in titanium offretite is quoted as 3% in weight,[33] while in our simulations it amounts to 7.2%, calculated as percent in weight of TiO_2 on the total framework composition.

2. Computational Details and Systems

The Car−Parrinello ab initio molecular dynamics method,[31] which combines a classical molecular dynamics scheme for the nuclei with first-principles calculations of the forces via density functional theory,[34,35] has been adopted in this study. The valence electrons wave functions are expanded in a planewave basis set with a cutoff of 60Ry; the time step for the numerical integration of the equations of motion was 0.121 fs, and a fictitious mass of 500 au for the electronic wave functions coefficients was used. Norm-conserving nonlocal pseudopotentials[36,37] were used for Si, Ti, O, and H. For titanium the nonlinear core correction has been adopted;[38] the electron−electron interaction was calculated by use of a gradient-corrected density functional approximation.[39,40] Temperature was controlled by Nosé thermostats.[41]

The simulations were performed at room temperature, and after equilibration, data were collected for a time of ∼2 ps for the anhydrous Ti-SiOFF and ∼4 ps for the two hydrated systems.

Natural offretite has a hexagonal structure, with space group *P*6*m*.[32] Its framework contains three different cavities: hexagonal prism (or double 6-ring), cancrinite cage, and gmelinite cage. In all the performed calculations the unit cell was fixed to $a = 13.229$ Å and $c = 7.338$ Å as in other simulations of silica-rich offretite systems,[42,43] with one Al atom per cell.

In the unit cell there are two different tetrahedral crystallographic sites, namely, T_1 and T_2: exactly 12 T_1 sites, belonging to the hexagonal prism, and 6 T_2 sites, in the 6-ring of the gmelinite cage (see Figure 1).

In our simulations Ti occupies one of the 12 equivalent T_1 sites. However, experimental data are not available to support our choice. We did not check for the best (more stable) location of Ti, and all Ti-doped systems were simulated with Ti always in the same T_1 position. It should be stressed that also in the much more studied TS-1 titanium silicalite system, the occupancy of Ti in the various sites is not completely clarified yet.[10]

To try to define the role of the water on the coordination and the structure of the Ti center, two independent simulations for the hydrated system, of composition $[TiSi_{17}O_{36}]\cdot(H_2O)_2$, have been carried out. The starting positions of the two water molecules differentiate the two systems. In the first simulated system, A, the two water molecules are located in two different cages, one placed into the 12-ring channel and the other one inside the hexagonal prism. In the second system, B, both water molecules were positioned inside the 12-ring channel.

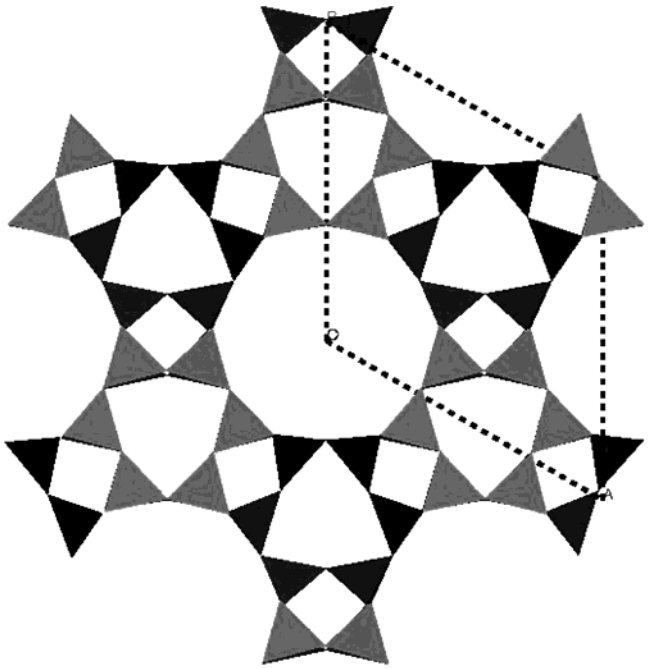

Figure 1. Polyhedral representation of the offretite system in the *ab* plane. The light gray tetrahedra refer to T_1 sites, and dark gray tetrahedra refer to the T_2 sites. The hexagonal elementary cell is indicated by dashed lines.

Moreover, a further ab initio molecular dynamics simulation of length of about 4 ps for an anhydrous, titanium-free all-silica $[Si_{18}O_{36}]$ offretite (SiOFF) has been performed, adopting the same cell parameters and computational approach above-reported, for comparison.

3. Results and Discussion

There are two T sites (T_1 and T_2) and six different crystallographic oxygen atoms (O_1–O_6) in the asymmetric unit of offretite.[32] The values of bond distances and angles referring to equivalent atoms are collected in Table 1. Reported bond distances and angles have been averaged over the trajectory and over equivalent positions in the unit cell. The calculated values for the various Ti-SiOFF are comparable with the ones calculated for the same sites in the reference all-silica offretite system (SiOFF). It is worth noting that, from the average quantities reported in Table 1, it is difficult to distinguish which site (T_1 or T_2) is occupied by titanium. Such a finding gives an indication of the problems[10] found in the experimental determination of Ti location in silicalite, where, moreover, there are 12 different T sites.

The values of Ti−O distances and O−Ti−O and Ti−O−Si angles are reported in Table 2. There is a remarkable increase of the Ti−O bond lengths compared to the Si−O ones. This causes slight and local deformations to the offretite framework. As reported in Table 2B, the average O−Ti−O angle is 109.4° for the water-free system, very close to the value obtained for site T_1 in the Ti-free system and very close to the ideal value of a tetrahedron. Also, our results are in qualitative agreement with previous calculations,[12,24,28] where a moderate distortion from the ideal tetrahedron geometry is reported for Ti sites; however, it is relevant to note that such tetrahedral geometry is unaffected by temperature, at least up to our simulation

TABLE 1: Equivalent Sites Averaged Bond Distances and Angles Calculated for the Simulated Offretite Systems

	Si-OFF	Ti Si-OFF	Ti Si-OFF A	Ti Si-OFF B
	(A) T−O Bond Distances (Å)			
T_1-O_1	1.630	1.628	1.628	1.634
T_1-O_2	1.644	1.644	1.645	1.641
T_1-O_3	1.635	1.635	1.632	1.635
T_1-O_4	1.625	1.627	1.623	1.629
T_2-O_1 (2×)	1.637	1.635	1.632	1.637
T_2-O_5	1.638	1.637	1.633	1.639
T_2-O_6	1.613	1.612	1.605	1.617
	(B) O−T−O Bond Angles (deg)			
$O_1-T_1-O_2$	110.8	110.9	110.3	110.6
$O_1-T_1-O_3$	109.8	109.6	109.3	109.4
$O_1-T_1-O_4$	106.7	106.8	106.9	106.7
$O_2-T_1-O_3$	108.2	108.1	108.0	108.7
$O_2-T_1-O_4$	110.8	110.8	111.4	111.0
$O_3-T_1-O_4$	110.2	110.3	111.0	110.1
$O_1-T_2-O_1$	110.0	110.2	110.2	109.5
$O_1-T_2-O_5$ (2×)	110.7	110.8	111.0	111.0
$O_1-T_2-O_6$ (2×)	108.0	107.8	107.6	107.9
$O_5-T_2-O_6$	109.0	109.1	108.7	109.1
	(C) T−O−T Bond Angles (deg)			
$T_1-O_1-T_2$	140.8	140.9	136.7	138.8
$T_1-O_2-T_1$	141.2	141.1	139.8	142.8
$T_1-O_3-T_1$	138.0	137.3	138.5	139.5
$T_1-O_4-T_1$	153.7	153.6	155.7	153.5
$T_2-O_5-T_2$	146.3	144.5	148.0	144.2
$T_2-O_6-T_2$	165.3	159.1	163.2	159.5

TABLE 2: Calculated Bond Distances and Angles for the Simulated Titanium Offretite Systems: Anhydrous Ti-SiOFF, Ti-SiOFF (System A), and Ti-SiOFF (System B)

	Ti Si-OFF	Ti Si-OFF A	Ti Si-OFF B
	(A) Ti−O Bond Distance (Å)		
$Ti-O_1$	1.820	1.820	1.857
$Ti-O_2$	1.831	1.829	1.862
$Ti-O_3$	1.830	1.836	1.854
$Ti-O_4$	1.803	1.803	1.813
avg Ti−O	1.821	1.822	1.846
	(B) O−Ti−O Bond Angles (deg)		
O_1-Ti-O_2	110.7	105.7	96.4
O_1-Ti-O_3	109.9	118.4	132.0
O_1-Ti-O_4	106.6	106.7	110.1
O_2-Ti-O_3	108.2	109.9	97.3
O_2-Ti-O_4	111.0	107.1	98.7
O_3-Ti-O_4	110.2	107.9	112.5
avg O−Ti−O	109.4	109.3	107.8
	(C) Ti−O−Si Bond Angles (deg)		
$Ti-O_1-T_2$	139.6	128.8	125.6
$Ti-O_2-T_1$	141.8	136.8	140.8
$Ti-O_3-T_1$	137.8	132.5	135.0
$Ti-O_4-T_1$	155.5	161.4	161.3

temperature of 300 K. The calculated average Ti−O bond lengths (1.821 Å) are larger than the distances of ∼1.8 Å generally obtained from energy optimizations in clusters or periodic systems.[7,24,28] They are, however, close to experimental results, e.g., 1.81 Å from XAFS data, as reported in ref 22. It should be noticed that bond lengths reported in the tables are obtained by averaging interatomic distances calculated at each configuration in the molecular dynamics trajectories; therefore, they include the contribution due to thermal motion.

Now, let us focus on the results of the hydrated systems. Simulation A, where the two water molecules are located in different cages, may well represent a situation of low water loading and guest molecules can be thought as isolated adsorbed molecules. By inspection of Table 2 it is possible to see that, in system A, the Ti center geometry is only moderately affected by the presence of water. Indeed, O−Ti−O bond angles and

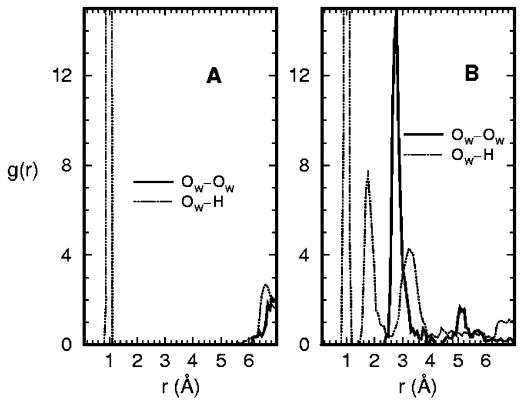

Figure 2. Water−water radial distribution functions calculated for systems A (on the left) and B (on the right). The solid line (O_w–O_w) refers to oxygen−oxygen pairs, and the dotted line (O_w–H) refers to oxygen−hydrogen pairs.

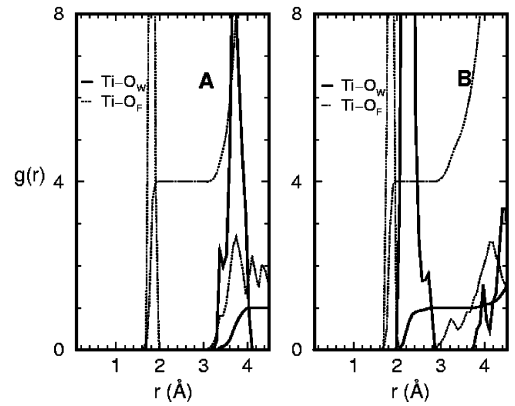

Figure 3. Calculated Ti−oxygen radial distribution function and Ti running coordination number. Solid lines (Ti−O_w) refer to Ti−water oxygen pairs, and dotted lines (Ti−O_F) refers to Ti−framework oxygen pairs. Functions calculated for system A are shown in the left panel, and those for system B are shown in the right panel.

Ti−O bond distances in the anhydrous Ti zeolite and in system A are very close. On the contrary, major changes have occurred in the geometry of the Ti center in simulation B. Large O−Ti−O angle variations, even if leading to an average value of 107.8° and an increase of the average bond length from 1.821 Å to 1.846 Å, are found for this system. Therefore, two water molecules in the same cavity (the large 12-ring channel) have produced a larger modification in the Ti center than two molecules in different cages. We have calculated the radial distribution functions (rdf) for relevant pairs of atoms. The water oxygen−water oxygen pair rdf and water oxygen−water hydrogen pair rdf for the two hydrated samples are reported in Figure 2: while in system A no water−water interaction is present, when water molecules are inside the same channel they interact and form a hydrogen-bonded pair. The calculated rdfs for Ti−$O_{framework}$ and Ti−O_{water} pairs are reported in Figure 3. In the same picture, the running coordination number of Ti, calculated from the integral of the corresponding rdf, is reported. While in system A the coordination for Ti is four (Ti is coordinated only by $O_{framework}$), in system B, a fifth oxygen (from a water molecule) is found in the coordination sphere of Ti, at an average distance of ∼2.22 Å. As we have imposed no constraints on the systems (apart from periodicity), it emerges that when two H_2O molecules can get close to each other to form a hydrogen-bonded dimer, than the oxygen of one water molecule seems activated and may enter the coordination shell

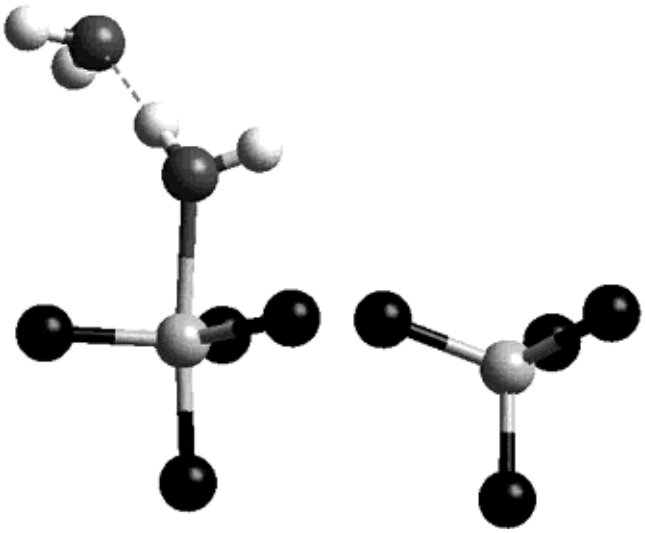

Figure 4. Ball-and-stick representation of the titanium center with its first neighbors in the two different Ti-SiOFF hydrated systems. On the left is reported the bipyramid structure found in system B, and on the right, the tetrahedral structure found in system A. The two configurations are represented with the same orientation. For system B (on the left) the hydrogen-bonded water pair is represented as well. Large black spheres represent framework oxygens, and large dark gray spheres represent water oxygens. Ti is represented by light gray spheres, and water's hydrogens are represented by small gray spheres. The hydrogen bond is sketched by a dashed line.

of Ti. To have an indirect proof of this last sentence, we simulated a system starting from a configuration from trajectory B and removing the water molecule far from Ti (the one not coordinated to Ti): in an elapsed time of 0.4 ps, the residual water molecule leaves the Ti shell and moves around in the large cavity while Ti changes its coordination from 5-fold to 4-fold (tetrahedral). A snapshot from systems A and B, representing the Ti center and its neighbor, is reported in Figure 4. It is clear that the geometry of the Ti coordination shell in system B is a distorted trigonal bipyramid, in line with previous calculations [see, e.g., ref 28]. However, a few points are worth noticing. The optimized water−Ti distance in ref 28 is 2.38 Å, and Ti−$O_{framework}$ distances are in the range 1.802−1.825 Å. On the other hand, we found a shorter average Ti−water distance (2.22 Å) and longer Ti−$O_{framework}$ (1.813−1.862 Å) bond lengths with respect to ref 28. Moreover, from our results, when H_2O is not activated, a pentacoordinated Ti complex seems unstable at room temperature with respect to H_2O still inside the zeolite but not linked to Ti.

This result is in apparent contrast with the finding of ref 28, where a binding energy of 25.1 kJ mol^{-1} for the formation of a pentacordinated Ti−CHA complex with a single, not activated, water molecule is reported. However, such a binding energy is calculated with respect to an isolated water molecule in a vacuum and not with respect to a water molecule inside the zeolite. Moreover, in standard MD simulations, while binding energies are not directly available, both energetic and entropic contributions are properly taken into account when statistical averages are performed. In this respect, it could be of relevance that a similar activation mechanism has been reported for the interaction of water with Brønsted acid sites in zeolites.[44−47]

The site−site (Si−Si and Si−Ti) radial distribution functions for the hydrated systems are reported in Figure 5, where, for comparison, the Si−Si rdf for the reference all-silica SiOFF system is reported as well. The Si−Si distributions are almost indistinguishable in the three different structures. The presence of a TiO_4 unit produces only local perturbations to the overall

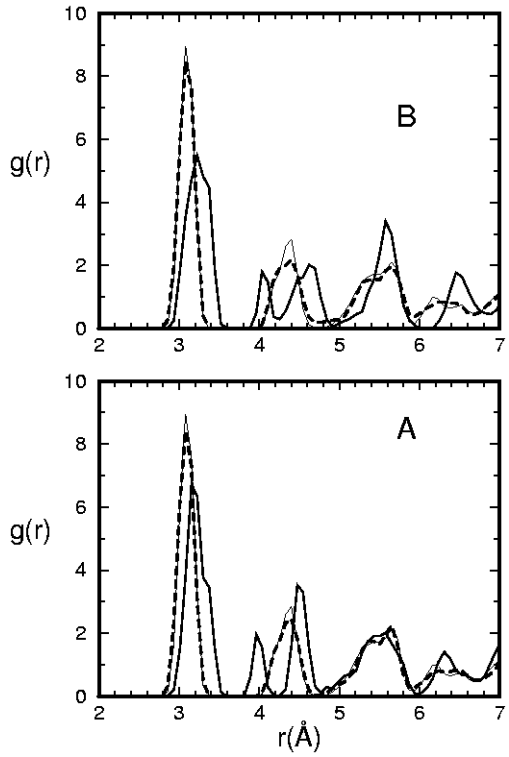

Figure 5. Calculated T−T radial distribution functions. The bottom panel refers to system A, while the top panel refers to system B. Thick dashed lines represent Si−Si pairs in the Ti-SiOFF systems. Thick solid lines represent Ti−Si pairs. The Si−Si rdf calculated for the Ti-free SiOFF system are represented as thin continuous lines in both panels.

Si−Si distribution, and such a perturbation is dependent on the water loading. It seems therefore that the average structure is only locally affected, and probably also the vibrational properties of the system will be moderately perturbed as well. Vibrational spectra can be obtained from MD simulations by Fourier-transforming correlation functions calculated from the time evolution of atomic positions or velocities in the system.[48]

The power spectra, i.e., the Fourier transforms of the velocity autocorrelation functions of the simulated systems, have been calculated for systems A and B and are reproduced in Figure 6, where the calculated power spectrum for all-silica offretite is reported for comparison. As in a Car−Parrinello MD, a fictitious mass is associated with the wave functions coefficients, the calculated frequencies for the atomic motion have to be scaled accordingly [see, e.g., ref 49]. In Figure 6 the region up to 1300 cm^{-1} is represented. The range from ∼900 to ∼1200 cm^{-1} is attributed to T−O−T asymmetric stretching modes, while that between ∼500 and ∼900 cm^{-1} is attributed to T−O−T symmetric stretching modes. The lower frequency region bands, below ∼500 cm^{-1}, are due to T−O−T bending modes and to more complex modes that are typical of the framework. The positions of the experimental (IR and Raman) Ti fingerprint bands at 960 and 1125 cm^{-1} are signalled by triangles in the picture.

First, let us briefly discuss the 890 cm^{-1} band, found in the SiOFF all-silica structure; indeed, this fact seems strictly related to the particular framework we are investigating and not to general features of Ti zeolites. We have found that this band is due to a symmetric Si−O−Si mode (involving O_1 oxygen). Such a band disappears in both Ti-SiOFF systems: it involves the T−O_1−T's whose angle shows the largest variation from Si−OFF to Ti-Si−OFF, as can be seen from Table 2C. As a general comment, it should be pointed out that with Ti-to-Si exchange,

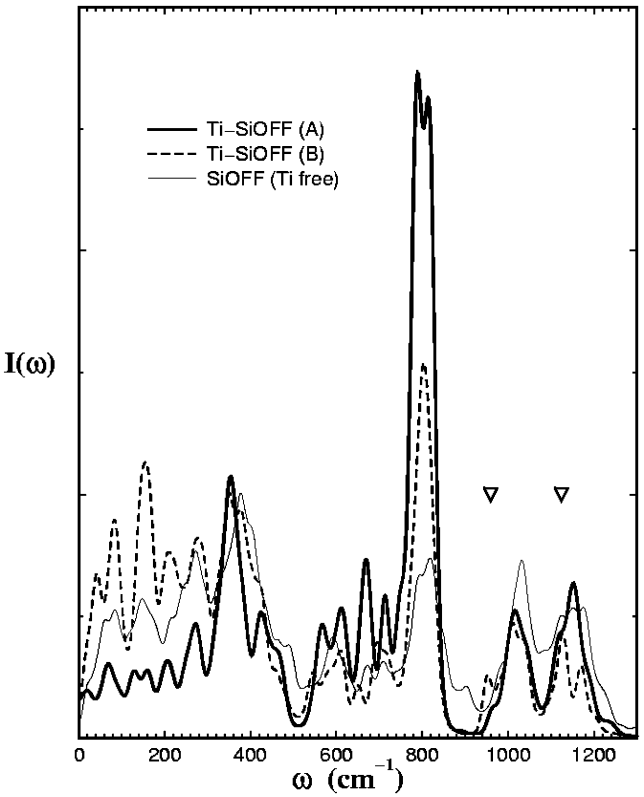

Figure 6. Calculated power spectra for the Ti-free SiOFF system (thin line), Ti-SiOFF system A (thick line), and Ti-SiOFF system B (dotted line). Triangles indicate the experimentally relevant frequencies 960 and 1125 cm^{-1}.

intertetrahedra angles (e.g., T−O−T ones) vary and such changes may imply modifications in the vibrational spectra.

In the 900−1200 cm^{-1} range it is possible to recognize a shoulder at 960 cm^{-1} for system A and a band at 940 cm^{-1} for system B, both missing in the parent Ti-free zeolite. Moreover, a peak at 1160 cm^{-1} in system A seems to disappear in system B.

From MD trajectories it is possible to single out the contributions (projections), to the total spectrum, of single atoms or groups of atoms, and we have found it convenient to analyze the contributions of the T−O−T modes. In particular, the various contributions to the asymmetric T−O−T stretching modes (a-s), all found at wavenumbers higher than 900 cm^{-1}, have been singled out, by separately calculating a-s modes for three group of TOTs, as a function of the distances from the Ti center: (i) Ti−O−Si modes, (ii) Si−O−Si modes due to a Si connected to Ti via one oxygen bridge, and finally (iii) the Si−O−Si modes involving Si not connected to Ti.

The results of the calculated projections for the hydrated systems A and B are reported in Figure 7 along with the corresponding total power spectra. It is evident from inspection of Figure 7 that the ∼960 cm^{-1} band can be assigned to a-s T−O−T modes due to Ti or Si connected to Ti and its contribution grows from system A (where it is found at ∼940 cm^{-1}) to system B. Another interesting point emerges by analyzing the 1120−1170 cm^{-1} region, where, in the total spectrum of system A, we have found a semitransparent window (low intensity). In system B, such a window is filled and a strong peak at 1135 cm^{-1} is present. From the analysis of the partial spectra, such a peak is assigned to a-s Si−O−Si modes primarily involving Si connected to Ti but not involving directly Ti−O−Si modes.

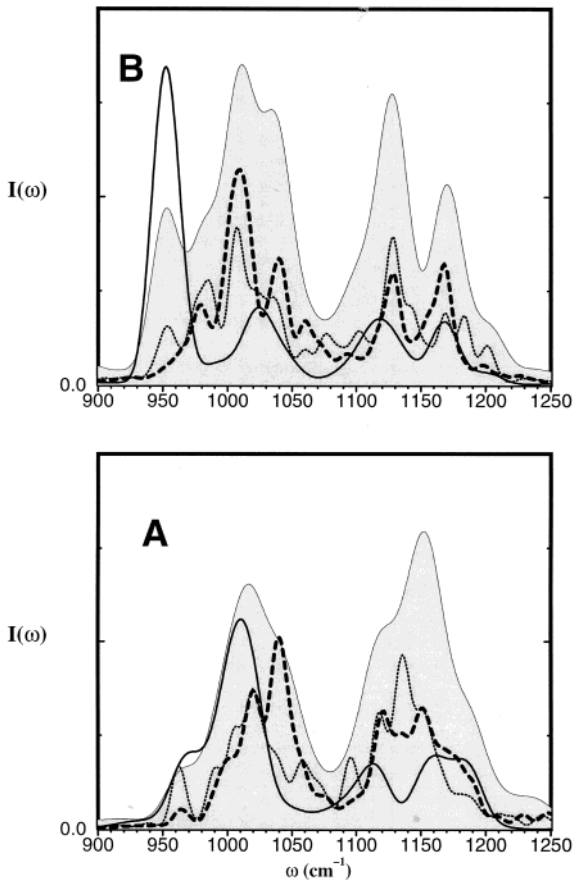

Figure 7. Calculated contributions to the total power spectrum of the asymmetric T−O−T stretching modes for system A (top panel) and system B (bottom panel). The solid line refers to the a−s Ti−O−Si modes, the dotted line to the Si−O−Si first neighbors of titanium, and the dashed line to the other a−s Si−O−Si modes. The shadow profile refers to the calculated total power spectra of the respective structure.

4. Conclusions

In this work we report on room-temperature structural and vibrational properties of a Ti center in offretite as studied via a first-principles molecular dynamics approach at fixed volume, number of particles, and temperature. Isomorphous Ti/Si exchange leads to a stable TiO_4 tetrahedron in a SiO_4 framework. As the volume of the TiO_4 is larger than the SiO_4 ones, distortions of intertetrahedra angles (T−O−T) are evident from the calculations; however, zeolites have good microscopic flexibility in order to bear such a modification.[50,51] For sake of completeness we must say that also a cell variation may result from heteroatom insertion even at low concentration; however, due to the high computational cost, we have not investigated the release of such a degree of freedom. From our results it is possible to say that the introduction of a larger tetrahedron implies a variation of the T−O−T angles distribution whose average is, however, moderate (see Tables 1C and 2C) and it means that an increase of a particular T−O−T angle at a distance *r* from the perturbing Ti center is largely compensated by the decrease of a second T−O−T bond angle at the same distance *r* from Ti. Moreover, such a perturbation is more pronounced in the neighborhood of the perturbing Ti site.

Upon water loading, two different behaviors have been detected. At low water loading (no interwater interaction), the TiO_4 tetrahedron is scarcely affected by guest molecules. On the other hand, at higher water loading, when interwater interactions are present, water molecules interact with Ti;

actually it is a water dimer that coordinates the Ti center, through the oxygen of the proton donor moiety in the hydrogen-bonded complex, namely, the oxygen that has full availability of its lone pairs and that is polarized by the companion H_2O molecule. Ti becomes pentacoordinated, with the water molecules at an equilibrium distance of 2.22 Å, and assumes a trigonal bipyramidal structure together with the four oxygens from the framework. The interwater hydrogen bond resulting is essential for the stability of the Ti−H_2O complex in offretite.

The structural modifications associated with the H_2O−Ti−OFF adduct formation are detectable in the calculated vibrational properties. The Ti tetra-to-pentacoordination transformation is revealed by a red shift (from 960 to 940 cm^{-1}) of a band localized on the Ti−O−Si a-s modes and a decrease in intensity of a band at 1135 cm^{-1} assigned to Si−O−Si a-s modes due to Si connected to Ti via a single oxygen bridge (we may represent them as [TiO]−Si−O−Si). These features may allow us a link with experimental data concerning TS-1. Indeed we have found that relevant vibrational aspects are due to modes derived from groups very close to the Ti center, and probably the framework topology may play a secondary role with respect to these properties. Actually, for TS-1 it is reported that, by increasing water loading, a red shift of the 960 cm^{-1} band is observed in both IR and Raman experiments, along with an intensity decrease of a 1125 cm^{-1} (Raman) band [see, e.g., ref 17], in fair agreement with our first-principles results, and the presented structural data may be used as a ground for the interpretation of the various facets obtained from experiments on TS-1.

The fact that we found that only "activated" water is able to influence the Ti coordination may be peculiar to T_1 sites in offretite; however, the point is that the different structural and dynamical properties calculated for tetracoordinated and pentacoordinated Ti sites may be not peculiar to offretite only. This is possible if Ti produces just local perturbations to a stable SiO_2 framework, as we have shown, for example, by the invariance of Si−Si rdfs. A possible rationale for such a statement can be found in the RUM (rigid unit modes) theory[50,51] for framework materials such as zeolites. The RUM theory explains the flexibility of such materials with low energy modes found in the intertetrahedra junctions (e.g., the T−O−T angles) that allow for zero-frequency deformations induced, for example, by diffusing ions or molecules and also by the presence of a larger and even deformed tetrahedron.

References and Notes

(1) Tamarasso, M.; Perego, B.; Notari, B. U.S. Patent 4410501, 1983.
(2) Clerici, M.; Ingallina, P. *J. Catal.* **1993**, *140*, 71.
(3) Notari, B. *Catal. Today* **1993**, *18*, 163.
(4) Vayssilov, G. N. *Catal. Rev. Sci. Eng*. **1997**, *39*, 209.
(5) Galli, E.; Gottardi, G. *Natural Zeolites*; Springer-Verlag: Berlin, Germany, 1985.
(6) Millini, R.; Perego, G. *Gazz. Chim. Ital.* **1996**, *126*, 133.
(7) Sinclair, P. E.; Sankar, G.; Catlow, C. R. A.; Thomas, J. M.; Maschemeyer, T. *J. Phys. Chem. B* **1997**, *101*, 4232.
(8) Lamberti, C.; Bordiga, S.; Arduino, D.; Zecchina, A.; Geobaldo, F.; Spanò, G.; Genoni, F.; Petrini, G.; Carati, A.; Villain, F.; Vlaic, G. *J. Phys. Chem. B* **1998**, *102*, 6382.
(9) Blasco, T.; Camblor, M. A.; Corma, A.; Pèrez-Pariente, J. *J. Am. Chem. Soc.* **1993**, *115*, 11806.
(10) Lamberti, C.; Bordiga, S.; Zecchina, A.; Artioli, G.; Marra, G. L.; Spanò, G. *J. Am. Chem. Soc.* **2001**, *123*, 2204.
(11) Zecchina, A.; Bordiga, S.; Lamberti, C.; Ricchiardi, G.; Lamberti, C.; Ricchiardi, G.; Scarano, D.; Petrini, G.; Leonfanti, G.; Mantegazza, M. *Catal. Today* **1996**, *32*, 97.
(12) Damin, A.; Bonino, F.; Ricchiardi, G.; Bordiga, S.; Zecchina, A.; Lamberti, C. *J. Phys. Chem. B* **2002**, *106*, 7524.
(13) Bordiga, S.; Damin, A.; Bonino, F.; Zecchina, A.; Spanò, G.; Rivetti, F.; Bolis, V.; Prestipino, C.; Lamberti, C. *J. Phys. Chem. B* **2002**, *106*, 9892.
(14) Lin, W.; Frei, H. *J. Am. Chem. Soc.* **2002**, *124*, 9292.
(15) Bolis, V.; Bordiga, S.; Lamberti, C.; Zecchina, A.; Crati, A.; Rivetti, F.; Spanò, G.; Petrini, G. *Langmuir* **1999**, *15*, 5753.
(16) Bordiga, S.; Coluccia, S.; Lamberti, C.; Marchese, L.; Zecchina, A.; Boscherini, F.; Buffa, F.; Genoni, F.; Leonfanti, G.; Petrini, G., Vlaic, G. *J. Phys. Chem.* **1994**, *98*, 4125.
(17) Ricchiardi, G.; Damin, A.; Bordiga, S.; Lamberti, C.; Spanò, G.; Rivetti, F.; Zecchina, A. *J. Am. Chem. Soc.* **2001**, *123*, 11409.
(18) Bellussi, G.; Carati, A.; Clerici, M. G.; Maddinelli, G.; Millini, R. *J. Catal*. **1992**, *133*, 220.
(19) Khouw, C. B.; Dartt, C. B.; Labinger, J. A.; Davis, M. E. *J. Catal*. **1994**, *149*, 195.
(20) Arends, I. W. C. E.; Sheldon, R. A.; Wallau, M.; Schuchardt, U. *Angew. Chem., Int. Ed. Engl.* **1994**, *36*, 1144.
(21) Tozzola, G.; Mantegazza, M. A.; Ranghino, G.; Petrini, G.; Bordiga, S.; Ricchiardi, G.; Lamberti, C.; Zulian, R.; Zecchina, A. *J. Catal.* **1998**, *179*, 64.
(22) Bordiga, S.; Coluccia, S.; Lamberti, C.; Marchese, L.; Zecchina, A.; Boscherini, F.; Buffa, F.; Genoni, F.; Leonfanti, G.; Petrini, G.; Vlaic, G. *J. Phys. Chem.* **1994**, *98*, 4125.
(23) De Man, A. J. M.; Sauer, J. *J. Phys. Chem.* **1996**, *100*, 5025.
(24) Damin, A.; Bordiga, S.; Zecchina, A.; Lamberti, C. *J. Chem. Phys*. **2002**, *117*, 226.
(25) Sinclair, P. E.; Catlow, C. R. A. *J. Phys. Chem. B* **1999**, *103*, 1084.
(26) Vayssilov, G. N.; van Santen, R. A. *J. Catal*., **1998**, *175*, 170.
(27) Zicovich-Wilson, C. M.; Dovesi, R.; Corma, A. *J. Phys. Chem. B* **1999**, *103*, 988.
(28) Damin, A.; Bordiga, S.; Zecchina, A.; Doll, K.; Lamberti, C. *J. Chem. Phys*. **2003**, *118*, 10183.
(29) Ricchiardi, G.; de Man, A.; Sauer, J. *Phys. Chem. Chem. Phys*. **2000**, *2*, 2195.
(30) Flanigen, E. M.; Bennett, J. M.; Grose, R. W.; Cohen, J. P.; Patton, R. L.; Kirchner, R. M.; Smith, J. V. *Nature* **1978**, *271*, 512.
(31) Car, R.; Parrinello, M. *Phys. Rev. Lett*. **1985**, *55*, 2471.
(32) Mortier, W. J.; Pluth, J. J.; Smith, J. V. *Z. Kristallogr*. **1976**, *143*, 319.
(33) Kwak, J. H.; Cho, S. J.; Ryoo, R. *Catal. Lett*. **1996**, *37*, 217.
(34) Kohn, W.; Sham, L. J. *Phys. Rev. A* **1965**, *140*, 1133.
(35) Perdew, J. P.; Zunger, A. *Phys. Rev. B* **1981**, *23*, 5048.
(36) Kleinman, L.; Bylander, D. M. *Phys. Rev. Lett*. **1982**, *48*, 1425.
(37) Troullier, N.; Martins, J. L. *Solid State Commun.* **1990**, *74*, 613−616.
(38) Louie, S. G.; Froyen, S.; Cohen, M. L. *Phys. Rev. B* **1982**, *26*, 1738.
(39) Becke, A. D. *Phys. Rev. A* 1**988**, *38*, 3098−3100.
(40) Perdew, J. P. *Phys. Rev. B* **1986**, *33*, 8822−8824.
(41) Nosé, S. *Mol. Phys.* **1984**, *52*, 255.
(42) Campana, L.; Selloni, A.; Weber, J.; Goursot, A. *J. Phys. Chem*. **1997**, *101*, 9932.
(43) Campana, L.; Selloni, A.; Weber, J.; Goursot, A. *J. Phys. Chem*. **1995**, *99*, 16351.
(44) Limtrakul, J.; Chuichay, P.; Nobkin, S. *J. Mol. Struct*. **2001**, *560*, 169.
(45) Wakabayashi, F.; Kondo, J. N.; Domen, K.; Hiros, C. *J. Phys. Chem.* **1996**, *100*, 1442.
(46) Lee, B.; Kondo, J. N.; Domen, K.; Wakabayashi, F. *J. Mol. Catal*. **1996**, *137*, 269.
(47) Krossner, M.; Sauer, J. *J. Phys. Chem*. **1996**, *100*, 6199.
(48) Madden, P. A. In *Liquids, Freezing and Glass Transition*; Hansen, J. P., Ed.; Elsevier: Amsterdam, 1991; pp 548−627.
(49) Tangney, P.; Scandolo, S. *J. Chem. Phys.* **2002**, *116*, 14.
(50) Hammond, K. D.; Deng, H.; Heine, V.; Dove, M. T. *Phys. Rev. Lett.* **1997**, *78*, 3701.
(51) Hammond, K. D.; Heine, V.; Dove, M. T. *J. Phys. Chem. B* **1998**, *102*, 1759.